

Characterization and localization of the cytoplasmic dynein heavy chain in *Aspergillus nidulans*

XIN XIANG, CHRISTIAN ROGHI, AND N. RONALD MORRIS*

University of Medicine and Dentistry of New Jersey–Robert Wood Johnson Medical School, Department of Pharmacology, 675 Hoes Lane, Piscataway, NJ 08854-5635

Communicated by Aaron J. Shatkin, Center for Advanced Biotechnology and Medicine, Piscataway, NJ, July 3, 1995 (received for review May 9, 1995)

ABSTRACT Migration of nuclei throughout the mycelium is essential for the growth and differentiation of filamentous fungi. In *Aspergillus nidulans*, the *nudA* gene, which is involved in nuclear migration, encodes a cytoplasmic dynein heavy chain. In this paper we use antibodies to characterize the *Aspergillus* cytoplasmic dynein heavy chain (ACDHC) and to show that the ACDHC is concentrated at the growing tip of the fungal mycelium. We demonstrate that four temperature-sensitive mutations in the *nudA* gene result in a striking decrease in ACDHC protein. Cytoplasmic dynein has been implicated in nuclear division in animal cells. Because the temperature-sensitive *nudA* mutants are able to grow slowly with occasional nuclei found in the mycelium and are able to undergo nuclear division, we have created a deletion/disruption *nudA* mutation and a tightly downregulated *nudA* mutation. These mutants exhibit a phenotype very similar to that of the temperature-sensitive *nudA* mutants with respect to growth, nuclear distribution, and nuclear division. This suggests that there are redundant backup motor proteins for both nuclear migration and nuclear division.

Cytoplasmic dynein is a minus-end-directed, microtubule-dependent motor protein that has been functionally implicated in organelle motility, mitosis in mammalian cells, and nuclear migration in fungi (1). In the filamentous fungus *Aspergillus nidulans*, several temperature-sensitive (ts) nuclear distribution (*nud*) mutants, including the *nudA*, *nudF*, and *nudC* mutants, have been isolated and their genes have been cloned by complementation of the mutant phenotype. *nudF* encodes a 49-kDa WD-repeat protein, NUDF, whose amino acid sequence is 42% identical to that of the human LIS1 protein, which is required for neuronal migration during brain development (2). *nudC* encodes a 22-kDa protein whose function is connected with that of the NUDF protein (2, 3). *nudA* encodes a cytoplasmic dynein heavy chain (CDHC) (4). Four recessive ts mutations of the *nudA* gene have been identified. All four block nuclear migration into the mycelium but have no apparent effect on nuclear division. Since cytoplasmic dynein plays a role in mitosis in higher eukaryotes, why the *nudA* mutations have no effect on mitosis in *A. nidulans* poses an interesting problem. As the *nud* phenotype by definition specifies clusters of nuclei, the *nud* mutations may have been selected as mutations that affect nuclear migration but that specifically do not affect nuclear division. Thus, the possibility exists that a complete loss of *nudA* function might give rise to a mitotic block similar to that seen in mammalian cells after injection of dynein antibody.

To address this problem and to initiate the biochemical analysis of the *A. nidulans* cytoplasmic dynein complex, we have made a strain ($\Delta nudA$) in which the four ATP-binding sites of the heavy chain are deleted and another strain

(*alcA(p)::nudA*) in which the only copy of the *nudA* gene is under the control of the inducible/repressible *alcA* promoter. We have generated an antibody against the N-terminal region of the NUDA protein and have used it to identify the CDHC by Western blotting and to characterize its location within the cell by immunocytochemistry in wild-type and mutant strains of *A. nidulans*.

MATERIALS AND METHODS

Aspergillus Strains, Growth Media, and Transformation.

The strains used were AO1 (*nudC3*; *pabaA1*; *wA2*; *nicA2*; *pyrG89*), XX3 (*nudA1*; *chaA1*; *pyrG89*), XX5 (*nudA2*; *pyrG89*; *wA2*; *chaA1*), XX8 (*nudA4*; *pyrG89*; *wA2*; *chaA1*), XX10 (*nudA5*; *pyrG89*; *wA2*; *chaA1*), XX20 (*nudF6*; *pyrG89*), XX21 (*nudF7*; *pyrG89*; *yA2*), SJ002 (*pyrG89*), GR5 (*pyrG89*; *pyroA4*; *wA2*), R153 (*pyroA4*, *wA2*), XX60 ($\Delta nudA::pyrG$; *pyrG89*), and XX61 [*alcA(p)::nudA::pyr4*; *pyrG89*; *pyroA4*; *wA2*]. Procedures for *Aspergillus* growth and transformation were performed as described (2, 5).

DNA Techniques. Cloning was performed by standard methods (6). Polymerase chain reactions (PCR) were performed with Vent polymerase (New England Biolabs). *A. nidulans* genomic DNA was isolated as described (7). Southern hybridizations were performed as described (2).

Molecular Disruption of *nudA*. We constructed a strain, $\Delta nudA$, in which the *nudA* gene was disrupted by replacing the nucleotide sequence coding for the four ATP binding sites (aa 1929–2965 of CDHC) with the orotidine-5'-phosphate decarboxylase gene (*pyrG*) (7). We first constructed a $\Delta nudA$ plasmid (pXX2) in which the *pyrG* gene was inserted between the upstream and the downstream flanking sequences of the region encoding the *A. nidulans* CDHC (ACDHC) ATP binding sites (Fig. 1A). This $\Delta nudA$ plasmid was constructed as follows. The 2-kb upstream flanking region of the first ATP binding site was amplified by PCR using the oligonucleotides K3U-KpnI (5' GCCCCGGTACCAGTTCCCTAGTG 3') and K3R-BamHI (5' CCCGGATCCAAGTCTTTGGCATAAAGGC 3') as primers (the recognition sites for the restriction endonucleases are underlined). The PCR product was digested with *Bam*HI and *Kpn*I to create the *Bam*HI–*Kpn*I fragment (fragment A). The 2.3-kb downstream flanking region of the fourth ATP binding site was amplified by PCR using the oligonucleotides 2.3R-SmaI (5'-TTTTCCCGGGTTTGA-CAAGATCAGAACG-3') and 2.3U-EcoRI (5'-GGTT-GAATTCAGACTTCGATGATGACC-3') as primers (the recognition sites for the restriction endonucleases are underlined). The PCR product was digested with *Sma*I and *Eco*RI to create the *Sma*I–*Eco*RI fragment (fragment B). The 1.5-kb *Sca*I–*Bam*HI fragment from the *pyrG* selectable marker gene (7) was ligated to the *Sma*I–*Bam*HI sites of pBluescript SK

The publication costs of this article were defrayed in part by page charge payment. This article must therefore be hereby marked "advertisement" in accordance with 18 U.S.C. §1734 solely to indicate this fact.

Abbreviations: CDHC, cytoplasmic dynein heavy chain; ACDHC, *Aspergillus nidulans* CDHC; ts, temperature-sensitive; DAPI, 4',6'-diamidino-2-phenylindole.

*To whom reprint requests should be addressed.

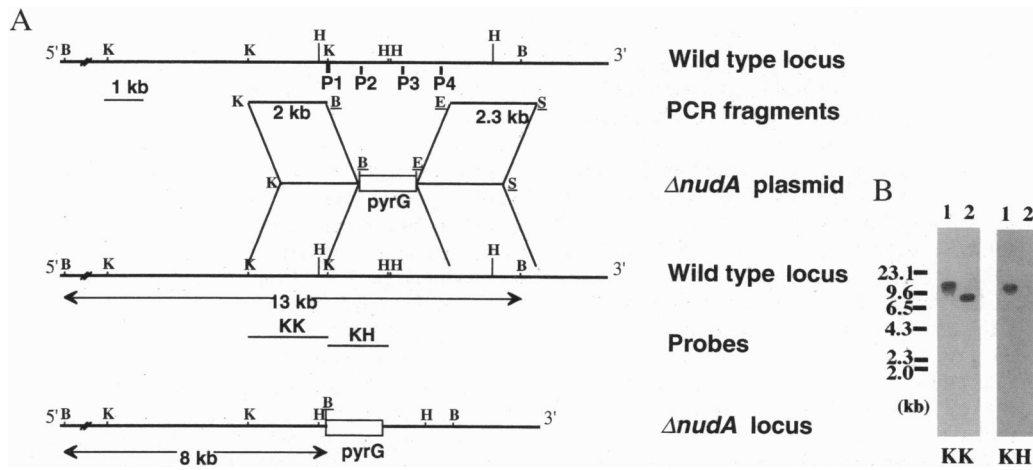


FIG. 1. Construction of the $\Delta nudA$ strain. (A) Illustration of the $\Delta nudA$ plasmid and the integration event that leads to the substitution of the *pyrG* marker gene for the region encoding the four ATP binding sites (P1–P4) of ACDHC. Underlined restriction sites were generated by PCR but are not present in the wild-type *nudA* locus (see *Materials and Methods*). B, *Bam*HI; E, *Eco*RI; H, *Hind*III; K, *Kpn* I; S, *Sma* I. (B) Southern blot demonstrating the integration of the $\Delta nudA$ plasmid into the *nudA* locus. Genomic DNA from the wild-type (lanes 1) and $\Delta nudA$ (lanes 2) strains was extracted and digested with *Bam*HI. Southern blot analysis of site-specific integration was performed with the KK and KH fragments as probes (see A). The KK probe detected a 13-kb signal in the wild-type strain and an 8-kb signal in the $\Delta nudA$ mutant, as predicted in A. The KH probe detected a 13-kb signal in the wild type but failed to detect any signal in the $\Delta nudA$ mutant, since the region containing this probe has been deleted in the $\Delta nudA$ strain.

(Stratagene) to create the plasmid pXX1. The *pyrG* gene was then excised from pXX1 as a *Bam*HI–*Eco*RI fragment (fragment C). Fragments A, B, and C were mixed together and ligated in a single ligation reaction to the *Kpn* I–*Sma* I sites of the pBluescript KS polylinker to make the $\Delta nudA$ recombinant plasmid pXX2.

The $\Delta nudA$ clone was digested by *Not* I and *Sma* I to produce a linearized fragment of the $\Delta nudA$ clone and transformed into *A. nidulans* wild-type strain SJ002. Transformants were streaked to single colony on YAG plates at 32°C. Slowly growing “nud”-like colonies were picked as potential $\Delta nudA$ strains. The site-specific integration of the $\Delta nudA$ sequence in the putative $\Delta nudA$ strain (XX60) was confirmed by Southern blot analysis (Fig. 1B).

Construction of a Conditionally “Null” *nudA* Mutant Strain. A 1.4-kb genomic DNA fragment beginning 100 bp upstream of the ATG start codon of *nudA* was amplified by PCR using the oligonucleotides nA-*Sma*I (5'-CCCCCCCCG-GAAAACCTCTATCTGCCCCG-3') and nA-*Bam*HI (5'-GGGGGGTACCCAGTCTTCATTAAGGTG-3') as primers (the recognition sites for the restriction endonucleases are underlined). The PCR product was digested with *Sma* I and *Bam*HI and then ligated into the *Sma* I–*Bam*HI sites of the pAL3 vector (8). The resulting *alcA*(p)::*nudA*5' plasmid

(pXX3) was transformed into *A. nidulans* wild-type strain GR5. The site-specific integration of the *alcA*(p)::*nudA*5' plasmid into the *nudA* locus generates a truncated *nudA* gene and a complete *nudA* gene and puts the intact copy of the *nudA* gene under the control of the *alcA* promoter (Fig. 2A). The transformed protoplasts were plated on minimal plates containing pyridoxine (0.5 mg/ml) with glycerol as the sole carbon source. Transformants were individually streaked to single colonies on glucose plates without NaCl to test the phenotypes. DNA was extracted from the nud-like colonies, and site-specific integration of the *alcA*(p)::*nudA*5' plasmid was confirmed by Southern analysis (Fig. 2B). The strain, in which the only copy of *nudA* is under the control of the *alcA* promoter, was designated *alcA*(p)::*nudA* (XX61).

Anti-ACDHC Antibody Preparation and Western Blotting. A 4.7-kb *Xho* I–*Hind*III fragment (5' of the first ATP binding site) that encodes a portion of the amino terminus of the ACDHC was ligated into the pUR291 vector (6), and the LacZ–NUDA fusion protein was induced as described (6). Inclusion bodies were isolated (6) and sent to Hazelton Research Products (Denver, PA) to make a rabbit polyclonal antiserum. A 3.1-kb *Bgl* II–*Bgl* II fragment from the 4.7-kb *Xho* I–*Hind*III region of the ACDHC sequence was ligated into pQE32 (Qiagen, Chatsworth, CA), and the His₆-tagged pro-

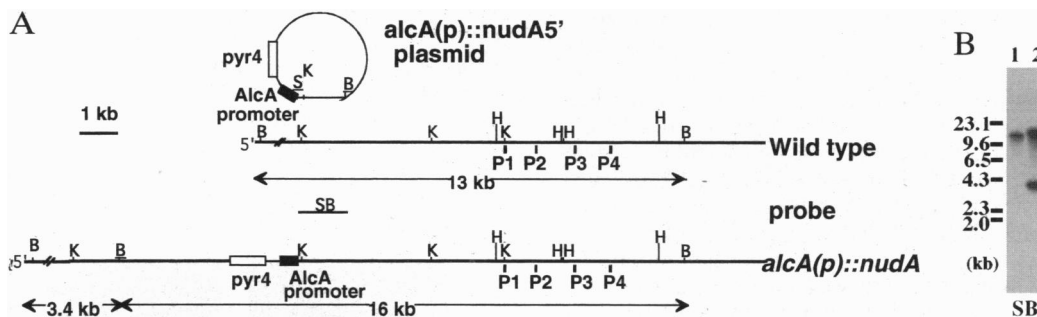


FIG. 2. Construction of the *alcA*(p)::*nudA* strain. (A) Illustration of the plasmid integration event that leads to a single copy of the full-length *nudA* gene under the control of the *alcA* promoter. Underlined restriction sites were generated by PCR but are not present in the wild-type *nudA* locus (see *Materials and Methods*). See Fig. 1A legend for abbreviations. (B) Southern blot demonstrating integration of the plasmid into the *nudA* locus. Genomic DNA from the wild-type (lane 1) and *alcA*(p)::*nudA* (lane 2) strains was extracted and digested with *Bam*HI. Southern blot analysis of site-specific integration was performed with the SB fragment as probe (see A). The SB probe detected a 13-kb signal in the wild-type DNA, and 3.4-kb and 16-kb signals in the mutant, as predicted in A.

tein was induced as described in the instructions for using the pQE vectors (Qiagen). The His₆-tagged protein was purified by following the instructions from Novagen and under denaturing conditions. The His₆-tagged protein was used to affinity purify the anti-ACDHC antibodies by the nitrocellulose absorption method (6).

Aspergillus protein preparation was performed as described (9) except that the ground mycelium was dispersed in protein extraction buffer containing 80 mM Pipes (pH 6.8), 1 mM EGTA, 1 mM MgCl₂, 1% (vol/vol) Nonidet P-40, 0.02% (wt/vol) sodium deoxycholate, and protease inhibitors (*N*^α-tosyl-L-arginine methyl ester, 1 mM; phenylmethylsulfonyl fluoride, 1 mM; leupeptin, 10 μg/ml; aprotinin, 10 μg/ml; pepstatin, 10 μg/ml). The protein samples were loaded on Mini-Protein II ready gels [4–15% polyacrylamide gradient gel, 0.375 M Tris-HCl (pH 8.8), Bio-Rad]. Western blotting was performed as described (6).

4',6-Diamidino-2-phenylindole (DAPI) Staining and Immunofluorescence. For nuclear staining of the germlings, 10⁶ asexual spores (uninucleate conidia) were inoculated onto coverslips in a Petri dish containing 30 ml of YG+UU medium. After 7 hr of incubation at 37°C, the cells were fixed and stained in 50 mM potassium phosphate, pH 6.6/0.2% (vol/vol) Triton X-100/5% (vol/vol) glutaraldehyde/0.025% DAPI; the coverslips were then washed twice in distilled water and mounted with Citifluor (Canterbury, Kent, U.K.).

For detection of cytoplasmic dynein by immunofluorescence, *A. nidulans* conidia were grown on sterile glass coverslips in YG+UU medium for 7 hr. The cells were fixed and processed as described (10) with the following modifications. The cell wall was digested for 1 hr at 28°C with a mixture containing 50% (vol/vol) egg white, 2 mM EGTA, 2.5% (wt/vol) driselase, 1% (wt/vol) lysing enzymes (L2265; Sigma), and protease inhibitors (aprotinin, 10 μg/ml; benzamide, 15.7 μg/ml; leupeptin, 10 μg/ml; pepstatin, 10 μg/ml; phenylmethylsulfonyl fluoride, 17.4 μg/ml; soybean trypsin inhibitor, 100 μg/ml; *N*^α-tosyl-L-arginine methyl ester, 10 μg/ml; and L-1-tosylamido-2 phenylethyl chloromethyl ketone, 10 μg/ml) (Sigma). The cells were extracted for 10 min at room temperature with 1% (vol/vol) Nonidet P-40 in extraction buffer and then incubated overnight at 4°C with affinity-purified anti-ACDHC antibodies were used at a 1:100 dilution in TBS (10) containing 3% (wt/vol) bovine serum albumin. After incubation with indocarbocyanine (Cy3)-conjugated goat anti-rabbit IgG (Jackson ImmunoResearch) at a dilution of 1:500, the coverslips were observed with a Zeiss epifluorescence microscope.

RESULTS AND DISCUSSION

The Deletion/Disruption Mutant of *nudA* Is Phenotypically Similar to the Original *ts nudA* Mutants. All four *ts nudA* mutants were able to grow slowly at restrictive temperature because occasional nuclei escaped the “nud” mutational block to migrate into the mycelium, where they continued to divide. To determine whether this “leakiness” reflects some residual low level of gene product that is able to support growth, and whether this residual gene product is also sufficient to support mitosis, we created a *nudA* null mutant strain, $\Delta nudA$, in which the *nudA* gene was disrupted by replacing the nucleotide sequence coding for the four ATP binding sites (aa 1929–2965 of ACDHC) with the *pyrG* gene, which encodes orotidine-5'-phosphate decarboxylase (7). First we constructed a plasmid in which the region coding for the four putative ATP binding sites of ACDHC was replaced by the selectable *pyrG* marker. This plasmid was then used to transform a *pyrG89* strain (Fig. 1A). Because *A. nidulans* is multinucleate, most transformants are initially heterokaryons (10) containing a mixture of transformed *pyrG*⁺/*nudA*⁻ nuclei and untransformed *pyrG*⁻/*nudA*⁺ nuclei. The two types of nuclei in the heterokaryon are

resolved upon the production of conidia (asexual spores), which are uninucleate. Both types of conidia are able to produce colonies in nonselective YG+UU medium (containing uracil and uridine), but only those with transformed (*pyrG*⁺/*nudA*⁻) nuclei can form colonies in YG medium (without uracil and uridine). In the putative $\Delta nudA$ transformant strain, two types of colonies, large and small, were observed in YG+UU medium, but only small colonies were observed on YG medium. When we observed the germinating spores at an early time point (about 7 hr), the transformant produced both wild-type and nud-like germlings on YG+UU, but only nud-like germlings on YG (Fig. 3). Southern blot analysis of DNA from this putative $\Delta nudA$ strain verified that the wild-type gene had been replaced by the $\Delta nudA$ sequence (Fig. 1B). The $\Delta nudA$ strain also was found to have a defect in nuclear migration (Fig. 3). The $\Delta nudA$ strain grows slowly as a nud-mutant-like colony and does not produce conidia at any temperature. The nud colony phenotype cosegregated with the inserted *pyrG* marker in a genetic cross. At 32°C, the radial growth rate of the $\Delta nudA$ strain is ≈20% that of the isogenic wild-type strain. Thus, despite the complete absence of functional CDHC, the $\Delta nudA$ mutant is still able to grow slowly. As in the *ts nudA* mutants, occasional nuclei are found in the mycelium, which presumably is the reason that the $\Delta nudA$ mutant colonies continue to grow slowly. This suggests that there is a low-level fail-safe system for nuclear migration in *A. nidulans*. We have sought but been unable to identify a second CDHC gene in *A. nidulans* by low-stringency hybridization. Therefore, it seems likely that such a system might be mediated by a different motor protein—e.g., kinesin.

Deletion/disruption of the ACDHC gene had no detectable effect on nuclear division. After 7 hr of incubation at 37°C, the $\Delta nudA$ cells contained a similar number of nuclei when compared with the wild-type cells (average of 11–12 nuclei per cell), suggesting that the disruption of the ACDHC gene does not affect mitosis. In *Saccharomyces cerevisiae* the kinesin-related proteins Cin8p and Kip1p are functionally redundant with cytoplasmic dynein with respect to mitosis (11). A similar redundancy might account for the lack of effect of CDHC gene disruption on mitosis in *A. nidulans*.

The $\Delta nudA$ strain also produced an important control for the antibody staining of gels and cells that allowed us to demonstrate unequivocally that the gel bands and cytoarchitectural structures stained by anti-ACDHC antibody contained authentic ACDHC. Because the $\Delta nudA$ strain did not make conidia (asexual spores), the usual starting material for cytological experiments, we made another strain, *alcA(p)::nudA*, to downregulate the amount of ACDHC in the cell. In this strain, the only copy of the *nudA* gene is under the control of the alcohol dehydrogenase I gene (*alcA*) promoter, which is repressed by growth on glucose (Fig. 2A). The strain construction was verified by Southern blot hybridization to show that the specific integration event occurred as expected (Fig. 2B). This strain grows like the wild type on glycerol medium, a nonrepressing medium. On glucose medium, the repressing medium, growth is inhibited and a nuclear migration defect is obvious (Fig. 3); however, as with the $\Delta nudA$ strain, there is no observable effect on nuclear division.

The Intracellular Level of CDHC Protein Is Decreased in the *nudA* Mutants. The *A. nidulans nudA* gene encodes a

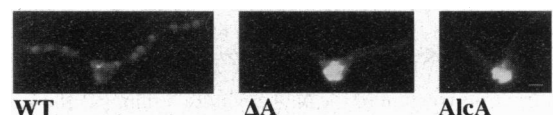


FIG. 3. Phenotype of the $\Delta nudA$ and *alcA(p)::nudA* mutants as shown by nuclear staining (with DAPI) of a wild-type cell (WT), a $\Delta nudA$ cell (ΔA) and an *alcA(p)::nudA* cell (AlcA) germinated at 37°C for 7 hr in glucose medium. (Bar = 5 μm.)

protein of 492.5 kDa. Western blotting of wild-type extracts of *A. nidulans* with affinity-purified antibodies against a fragment of the wild-type ACDHC stained a very high molecular weight protein consistent with the molecular weight of the ACDHC (Fig. 4A). To demonstrate the specificity of this reaction, we used protein extracts from the $\Delta nudA$ strain as well as the *alcA(p)::nudA* strain grown in glucose-containing medium as controls (Fig. 4B). In the $\Delta nudA$ strain and the *alcA(p)::nudA* strain grown on glucose, the high molecular weight signal disappeared. To examine whether the protein levels of the other *nud* gene products were affected in these *nudA* mutants, these Western blots were also probed with affinity-purified antibodies raised against two additional *nud* gene products, NUDF (2) and NUDC (3). Deletion/disruption or downregulation of the ACDHC gene had no obvious effect on the abundance of either NUDF or NUDC on Western blots (Fig. 4B). To determine whether the ACDHC protein level was affected by any of the other well-characterized *nud* mutations, we examined protein extracts from *nudA* (4), *nudF* (2), and *nudC* (3) mutants grown at restrictive temperature. The ACDHC protein level decreased dramatically in all four of the *nudA* mutants, but was not decreased by the *nudC3*, *nudF6*, and *nudF7* mutations (Fig. 5).

The four *ts nudA* mutants all have very low levels of intracellular ACDHC at restrictive temperature. This explains why these mutations exhibit a *nud* phenotype. These *ts* mutations can all be complemented by transformation with *nudA* coding sequences and therefore are located within the structural gene. A likely explanation for the effect of these mutations is that they either prevent proper folding of the ACDHC protein or inhibit the incorporation of ACDHC into the cytoplasmic dynein complex, so that the unfolded or unincorporated protein is degraded.

ACDHC Is Concentrated at the Tip of the Growing Germ Tube. We used affinity-purified anti-ACDHC antibodies to localize cytoplasmic dynein in *Aspergillus* cells. In wild-type cells, cytoplasmic dynein was concentrated at the tip of the germ tube (Fig. 6A and B). To confirm that the staining pattern reflects specifically the localization of the *nudA* gene product, we used the *alcA(p)::nudA* strain as a control. In *alcA(p)::nudA* cells grown on glucose medium, the tip staining disappeared (Fig. 6C and D). This observation is consistent with the marked decrease in ACDHC protein detected by Western blot analysis of extracts from cells grown on glucose.

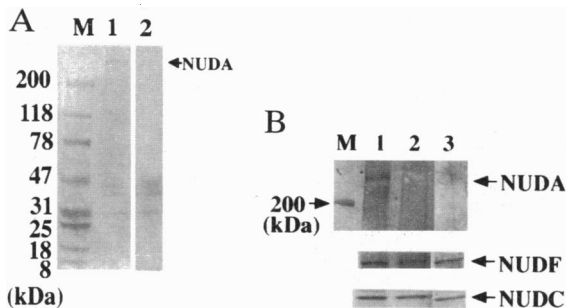


FIG. 4. Western blot analysis of the ACDHC protein. (A) The entire blot was probed with the affinity-purified anti-ACDHC antibodies (1:500). Lanes: M, molecular size markers; 1, wild-type extract; 2, same sample as lane 1, but probed with secondary antibody alone. (B) The upper part of the blot was probed with affinity-purified anti-ACDHC antibodies (1:500); the signal above the 200-kDa marker was detected only in the wild-type strain. The lower parts of the blot were probed with anti-NUDF (1:500) and anti-NUDC (1:2000) antibodies. Lanes: M, molecular size markers; 1, wild type; 2, $\Delta nudA$ strain; 3, *alcA(p)::nudA* strain. The wild-type and *alcA(p)::nudA* strains were grown on glucose medium for 42 hr. The inoculation was 10^7 cells per 200 ml for the wild type and 10^8 cells per 200 ml for the *alcA(p)::nudA* mutant. For the $\Delta nudA$ strain, pieces of mycelia were inoculated and allowed to grow for 4 days at 37°C.

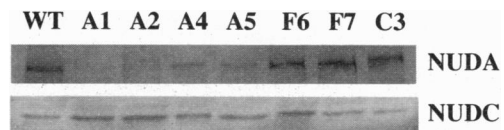


FIG. 5. Western blot analysis of the ACDHC protein level in various *nud* mutants. The wild-type strain and the mutant strains were grown at restrictive temperature for 42 hr. The inoculation was 10^7 cells per 200 ml for the wild type and 10^8 cells per 200 ml for the mutants. Thirty micrograms of protein was loaded in each lane. The blots were probed with affinity-purified anti-ACDHC antibodies (1:500) and anti-NUDC antibodies (1:2000) for 3 hr. WT, wild type; A1, *nudA1*; A2, *nudA2*; A4, *nudA4*; A5, *nudA5*; F6, *nudF6*; F7, *nudF7*; C3, *nudC3*.

It might be argued that this is simply the result of the slow growth phenotype of this or any *nud* mutation. To address this concern, we stained a conditional *alcA(p)::nudF* mutant down-regulated on glucose (2). This *alcA(p)::nudF* strain has the same phenotype as the *alcA(p)::nudA* strain under repressing conditions. The anti-ACDHC antibodies stained strongly at the tip in this strain (Fig. 6E and F), indicating that the decrease in the NUDF protein level (which produced a *nud* phenotype) did not abolish the tip staining that we observed in the wild-type cells. Together, these results demonstrate that the staining at the tip truly represents the ACDHC molecule.

Our immunofluorescence results may help to explain how cytoplasmic dynein mediates nuclear migration. Dynein behaves as a minus-end-directed motor in *in vitro* motility assays. Cytoplasmic dynein anchored in the mycelial tip could reel-in nuclei toward the tip by translocating toward the minus end of astral microtubules at the spindle pole body. This model was first suggested to explain nuclear migration into the bud in *S. cerevisiae* (12–14). Our results provide support for this model by showing that cytoplasmic dynein is concentrated at the growing tip.

Although the “dynein at the tip” model is attractive, it is unproven and incomplete. For example, much more informa-

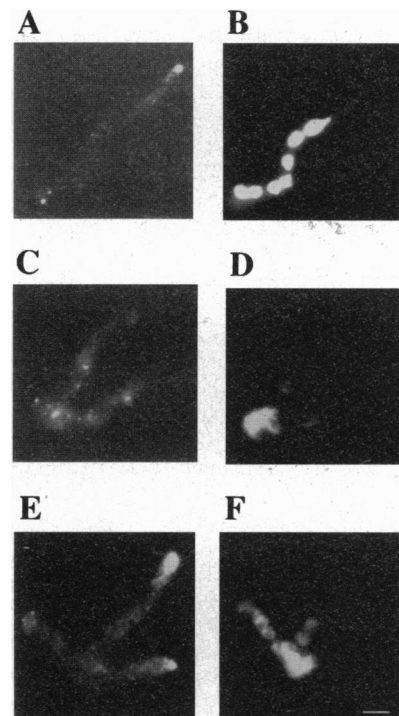


FIG. 6. ACDHC localization (A, C, and E) and DAPI staining (B, D, and F) of a wild-type cell (A and B), an *alcA(p)::nudA* cell (C and D), and an *alcA(p)::nudF* cell (E and F) germinated at 37°C for 7 hr in glucose medium. (Bar = 5 μ m.)

tion is needed about the polarity of cytoplasmic microtubules in fungi. An experiment in *Uromyces phaseoli* suggests that cytoplasmic microtubules may have their minus ends at the fungal tip (15), but this has not yet been confirmed. A second problem concerns the fact that there are multiple nuclei in the growing tip cell of *A. nidulans*. It has been proposed that nuclei are connected but separated by cytoplasmic dynein on interdigital microtubules (16). This model predicts that some molecules of cytoplasmic dynein should be localized to microtubules, which we did not see in our experiments. It is possible that the dynein molecules located on the microtubules are not sufficiently abundant to be detected.

The apex of the germ tube in filamentous fungi is a complex structure. Actin (17), myosin (18), and a collection of vesicles (19), which are implicated in tip growth, have been localized there. It will be very interesting to determine what structure(s) at the tip contain cytoplasmic dynein by EM studies.

The biochemical and cytological characterization of AC-DHC will allow further study of the regulation of dynein function. In mammalian cells the localization of CDHC to the membranous organelles is regulated by phosphorylation (20). Another large protein complex, the Glued/dynactin complex (21, 22), is required for dynein to move vesicles *in vitro* (23) and may be required to couple the CDHC to the vesicles. Mutations in components of this complex affect nuclear migration in fungi (16, 24, 25); however, it is not known whether dynein localization *in vivo* is dependent on an intact Glued/dynactin complex. We have characterized a large number of *nud* mutations in *A. nidulans*. With a combination of molecular genetic and cytological approaches, it should now be possible for us to identify those proteins that are required for localization of cytoplasmic dynein in living cells.

We thank the Morris lab members, especially Dr. S. Beckwith, Dr. D. Willins, Dr. B. Liu, M. Xin, and Y. Chiu, for constructive discussions and technical advice during this project. We are grateful to Dr. H. Geller for allowing us to use the microscope and the printer in his lab. This research was supported by the National Institute of General Medical Sciences.

1. Holzbaur, E. L. F. & Vallee, R. B. (1994) *Annu. Rev. Cell Biol.* **10**, 339–372.
2. Xiang, X., Osmani, A. H., Osmani, S. A., Xin, M. & Morris, N. R. (1995) *Mol. Biol. Cell* **6**, 297–310.
3. Osmani, A. H., Osmani, S. A. & Morris, N. R. (1990) *J. Cell Biol.* **111**, 543–551.
4. Xiang, X., Beckwith, S. & Morris, N. R. (1994) *Proc. Natl. Acad. Sci. USA* **91**, 2100–2104.
5. Osmani, S. A., May, G. S. & Morris, N. R. (1987) *J. Cell Biol.* **104**, 1495–1504.
6. Sambrook, J., Fritsch, E. F. & Maniatis, T. (1989) *Molecular Cloning: A Laboratory Manual* (Cold Spring Harbor Lab. Press, Plainview, NY), 2nd Ed.
7. Oakley, B. R., Rinehart, J. E., Mitchell, B. L., Oakley, C. E., Carmona, C. L., Gray, G. L. & May, G. S. (1987) *Gene* **61**, 385–399.
8. Waring, R. B., May, G. S. & Morris, N. R. (1989) *Gene* **79**, 119–130.
9. Mirabito, P. M. & Morris, N. R. (1993) *J. Cell Biol.* **120**, 959–968.
10. Osmani, S. A., Engle, D. B., Doonan, J. H. & Morris, N. R. (1988) *Cell* **52**, 241–251.
11. Saunders, W. S., Koshland, D., Eshel, D., Gibbons, I. R. & Hoyt, M. A. (1995) *J. Cell Biol.* **128**, 617–624.
12. Eshel, D., Urrestarazu, L. A., Vissers, S., Jauniaux, J.-C., van Vliet-Reedijk, J. C., Planta, R. J. & Gibbons, I. R. (1993) *Proc. Natl. Acad. Sci. USA* **90**, 11172–11176.
13. Li, Y.-Y., Yeh, E., Hays, T. & Bloom, K. (1993) *Proc. Natl. Acad. Sci. USA* **90**, 10096–10100.
14. Schroer, T. A. (1994) *J. Cell Biol.* **127**, 1–4.
15. Hoch, H. C. & Staples, R. C. (1985) *Protoplasma* **124**, 112–122.
16. Plamann, M., Minke, P. F., Tinsly, J. H. & Bruno, K. (1994) *J. Cell Biol.* **127**, 139–149.
17. Heath, I. B. (1990) *Int. Rev. Cytol.* **123**, 95–127.
18. McGoldrick, C. A., Gruver, C. & May, G. S. (1995) *J. Cell Biol.* **128**, 577–587.
19. Grove, S. N. & Bracker, C. E. (1970) *J. Bacteriol.* **104**, 989–1009.
20. Lin, S. X. H., Ferro, K. L. & Collins, C. A. (1994) *J. Cell Biol.* **127**, 1009–1019.
21. Gill, S. R., Schroer, T. A., Zilak, I., Steuer, E. R., Sheetz, M. P. & Cleveland, D. W. (1991) *J. Cell Biol.* **115**, 1639–1650.
22. Holzbaur, E. L. F., Hammarback, J. A., Paschal, B. M., Kravit, N. G., Pfister, K. K. & Vallee, R. B. (1991) *Nature (London)* **351**, 579–583.
23. Schroer, T. A. & Sheetz, M. P. (1991) *J. Cell Biol.* **115**, 1309–1318.
24. Muhua, L., Karpovar, T. S. & Copper, J. A. (1994) *Cell* **78**, 669–679.
25. Robb, M. J., Wilson, M. A. & Vierula, P. J. (1995) *Mol. Gen. Genet.* **247**, 583–590.